

## Analysis of L-mode turbulence in the MAST boundary plasma

<sup>1</sup>G.F. Counsell, <sup>2</sup>B. Ayed, <sup>1</sup>R. Dendy, <sup>3</sup>B. Dudson, <sup>4</sup>B. Hnat, <sup>1</sup>A. Kirk, <sup>1,5</sup>S. Lisgo, <sup>6</sup>T.D. Rognlien, <sup>7</sup>R. Scannell, <sup>8</sup>S. Tallents, <sup>6</sup>M.V. Umansky and <sup>6</sup>X.Q. Xu

<sup>1</sup>EURATOM/UKAEA Fusion Association, Culham Science Centre, Abingdon, Oxon, OX14 3DB UK

<sup>2</sup>University of York, Heslington, York YO10 5DD UK

<sup>3</sup>Department of Physics, University of Oxford, Parks Road, Oxford, OX1 3PU UK

<sup>4</sup>Centre for Fusion, Space and Astrophysics, Department of Physics, Warwick University, Coventry CV4 7AL U.K.

<sup>5</sup>University of Toronto Institute for Aerospace Studies, Toronto, M3H 5T6 Canada

<sup>6</sup>LLNL, Livermore, CA 94551 U.S.A

<sup>7</sup>Department of Electrical & Electronic Engineering, University College Cork, Association EURATOM-DCU Ireland.

<sup>8</sup>Imperial College, Prince Consort Road, London SW7 2BZ UK

E-mail: [glenn.counsell@ukaea.org.uk](mailto:glenn.counsell@ukaea.org.uk)

### Abstract

Turbulent transport in the edge of Ohmic and neutral beam heated L-mode plasmas on MAST has been diagnosed using Langmuir probes, an edge Thomson scattering system and a fast, 2D visible light camera and modelled using the BOUT two-fluid Braginskii code. Results suggest that electrostatic drift wave turbulence (ESDWT), 1 or 2 cm inside the separatrix and correlated for long timescales (several 100  $\mu$ s), generates density (and temperature) fluctuations in the plasma through turbulent mixing of eddies close to the separatrix. These fluctuations are then propelled into and across the scrape-off layer, primarily by curvature drive (i.e. interchange-like), where they appear as elongated plasma filaments with short timescale correlation (dispersing in  $\sim 30 - 60 \mu$ s). Close to the region of ESDWT, the turbulent fluctuations are symmetrically distributed around a mean and correlated for long timescales. Farther out in the SOL, the fluctuations are dominated by plasma filaments, which have a positively skewed distribution and short timescale correlations.

### 1. Introduction

Regimes with an L-mode edge remain an important candidate operating scenario for fusion power plants due to the absence of transient power loads associated with edge localised modes (ELMs), for which a sufficiently effective and reliable mitigation scheme has yet to be demonstrated. The cross-field transport of heat and particles in the scrape-off layer (SOL) of these plasmas is often represented in the leading edge fluid codes by poloidally and radially constant perpendicular diffusivities. The use of such a straightforward representation has historically been supported by experimental observations of a diffusive-like SOL from several diagnostic sources, for example target Langmuir probe arrays show an apparently 'exponential' decay in plasma properties across the SOL. Despite the simplicity of the approach to cross-field transport, the edge fluid codes have had considerable success in modelling many features of the phenomena observed to occur in the SOL and boundary plasma: divertor detachment; MARFE formation; the impact of target angle and so on. In recent years, however, new observations on a number of devices have been difficult to reproduce with the diffusive model. These include significant recycling at surfaces far from the plasma boundary and the detailed structure of flows in the SOL at a large fraction of the Mach number. One possible explanation currently being investigated is that intermittent convective transport, driven by radially propagating plasma structures, may play a key role in cross-field transport, modifying or even dominating diffusive-like processes, particularly in the far SOL (e.g. [1,2]).

Intermittent transport at the edge of L-mode plasmas on MAST has been investigated using Langmuir probes, an edge Thomson scattering system and 2D imaging in visible light. The data have been analysed to characterise the statistical nature of the intermittency and to

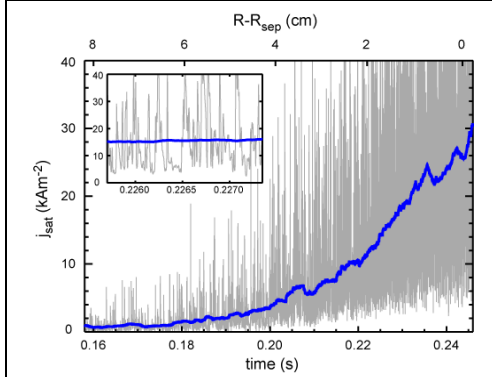


**Figure 1:** Particle flux to the MAST outboard mid-plane reciprocating probe during one sweep across the SOL in a 760kA Ohmic lower single null plasma with line averaged density of  $2.7 \times 10^9 \text{ m}^{-3}$ . The intermittent component to the signal dominates the underlying trend, represented by the overlaid, time averaged trace (blue).

apparent, however, that the characteristics of the intermittency change with distance from the separatrix. At low values of  $r$  ( $= R - R_{\text{sep}}$ ), the fluctuations are of the same order as the average value and are distributed evenly either side of the mean. At large  $r$ , the fluctuations have a smaller absolute magnitude but are much larger than, and predominantly above, the mean. These characteristics can best be demonstrated by taking the probability density function (PDF) of the signal at different values of  $r$ , as shown in figure 2. In this discharge, the probe was reciprocated during the flat-top phase of the plasma and penetrated beyond the separatrix to a depth of around 2cm, from a starting location at  $r \sim 4$  cm. The PDF of the data corresponding to  $r < -1$  cm is reasonably symmetrically distributed around the mean (at about  $9 \text{ kA/m}^2$ ). With increasing  $r$ , the mean value decreases but the PDF becomes progressively more skewed to values above the mean. Such behaviour has been noted on several tokamaks for L-mode conditions (e.g. [5]), and appears to hold whether the measured parameter is particle flux, density or temperature.

Beyond a radius of  $r \sim 1 - 2$  cm, the shape of the PDF in MAST changes little. This is confirmed by figure 3, which shows the skewness,  $S$  ( $= \sum_i^N (y_i - \bar{y})^3 / Ns^3$ , where  $\bar{y}$  is the mean and  $s$  the standard deviation) of the PDF as a function of  $r$ , both for the reciprocation shown in figure 2 and three similar shots in which the probe was held at fixed  $r$ .  $S$  is zero close to, and probably inside, the separatrix (there is typically an error of  $\sim 1$  cm in estimates of the mid-plane radius from equilibrium reconstruction in MAST, so it is difficult to say with certainty where deviation from zero begins). By  $\sim 2$  cm into the SOL, the rise flattens off at a value of  $\sim 2.5$ . Again, a similar trend and, in fact, similar values for  $S$  have been reported in the edge of many magnetically confined plasma devices; divertor ([6]) and limiter

obtain quantitative information on the size, shape, distribution and dynamics of the associated plasma structures. These analyses are compared with characteristics of edge turbulence derived from modelling of the MAST L-mode edge plasma using the BOUT two-fluid Braginskii code [4], which has been adapted to work in the double-null geometry typical of MAST plasmas.

## 2. Intermittency in the MAST SOL

Upstream SOL reciprocating probe data is often presented with either time or space averaging to show underlying trends (e.g. an ‘exponential’ fall-off in plasma parameters across the SOL). Analysis of the raw data, however, typically shows a highly intermittent characteristic and in MAST L-mode plasmas the fluctuating component at the outboard mid-plane dominates even close to the separatrix (figure 1). It is

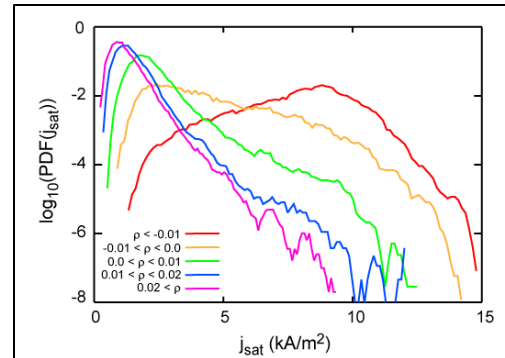


**Figure 2:** Probability density functions for fluctuations in the particle flux to a probe at different positions in the edge of a 925 kA double-null L-mode plasma with 1.2MW of neutral beam heating and a line average density of  $2.4 \times 10^9 \text{ m}^{-3}$ .  $r$  ( $= R - R_{\text{sep}}$ ) is in centimetres.

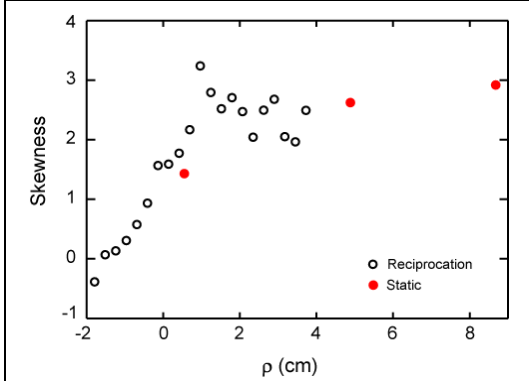


**Figure 3:** Variation in skewness of the PDF with edge location for the shot referred to in figure 2, in which a probe was reciprocated across the edge (open symbols), and three similar shots, in which the probe was held at static locations w.r.t. the separatrix

([7]) tokamaks, stellarators ([8]) and even devices without magnetic curvature ('linear' plasmas). This has led to edge intermittency being referred to as a 'universal' property ([9]).

Conditional averaging of fluctuations in particle flux to the probe reveals another change in character with increasing  $r$ . Fluctuations exceeding the mean by twice the standard deviation were selected and averaged. The result is shown in figure 4 for the three shots indicated by solid red circles in figure 3, at  $r = 0.5, 5$  and  $9$  cm. Several features are worthy of note. The amplitude of the 'spike' falls off with a  $1/e$  width of around  $3.5$  cm, the base level falls off more steeply,  $1/e \sim 2.5$  cm. The shape of the spikes at  $r = 5$  and  $9$  cm appears almost identical, with a steep rise and

shallow decay, whereas the spike at  $r = 0.5$  cm has a symmetric structure. In fact, the transition to an asymmetric spike takes place for  $r > \sim 2$  cm (from analysis of reciprocation data).

The change in the statistical properties and structure of the spikes with radius is suggestive that transport in the edge plasma may be governed by competition between more than one physical process. This hypothesis will be returned to in section 5, on modelling of the edge.

Analysis of the timescales for correlation of the intermittency using structure functions gives a further indication that multiple processes may be at play. The raw  $I_{sat}$  signal was summed across a window of width

$\tau$  [10,11] such that  $dx(t, \tau) = \sum_{t' = t}^{t + \tau} I_{sat}(t')$ . The statistical

properties of the higher order moments for  $\delta x(t, \tau)$  were analysed using generalised structure functions  $S_m(t) = \langle |dx(t, \tau)|^m \rangle$ , where  $m$  is real. The results of this analysis are shown in figure 5 for the first four moments,  $1 < m < 4$ , and clearly show that there are two distinct regions of scaling: Region I with a steeper slope extending from  $\tau \sim 2 \mu s$  to  $\tau \sim 60 \mu s$  and Region II with a shallower slope between scales  $\tau \sim 60 \mu s$  and  $\tau \sim 400 \mu s$ . PDFs constructed for data on temporal scales  $\tau \sim 10 \mu s$  and  $\tau \sim 80 \mu s$  (i.e. in Regions I and II respectively) are shown in figure 6. Interestingly, the short timescale data has a strongly skewed PDF similar to that for data at  $r > \sim 2$  cm (see figure 2), whilst that for the long timescale data is similar to the more symmetric distribution close to the separatrix. It is worth noting that these PDFs are well fitted by the single parameter, Fréchet and two parameter, Gumbel distributions for Region I and II respectively, but not particularly well by the more common log-normal and

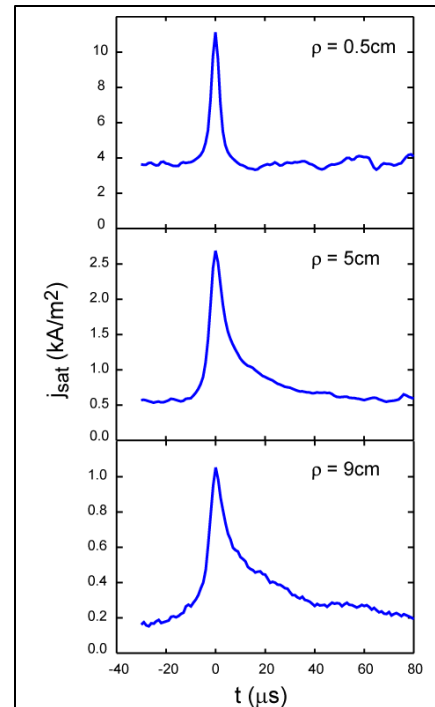
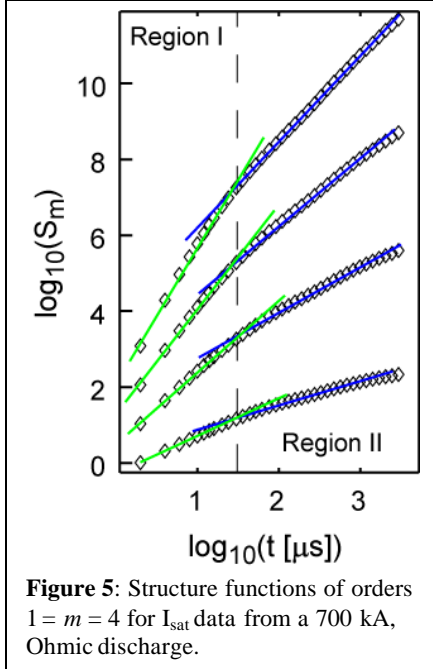


**Figure 4:** Conditionally averaged intermittent particle flux signals at three positions in the edge plasma (corresponding to the solid symbols in figure 3)

It is worth noting that these PDFs are well fitted by the single parameter, Fréchet and two parameter, Gumbel distributions for Region I and II respectively, but not particularly well by the more common log-normal and



Gaussian distributions. The Fréchet and Gumbel distributions both represent the largest events drawn from an underlying ensemble, whose PDF decays faster than a power law.

### 3. Analysis of L-mode filamentary structures in MAST

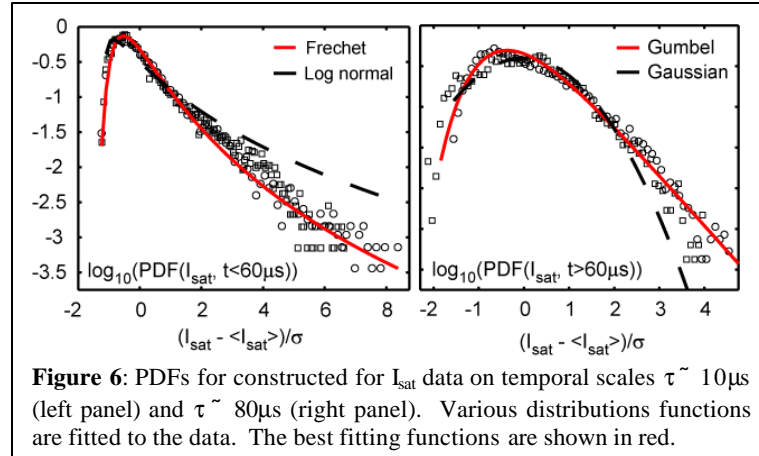
Fast, 2D imaging of the MAST plasma in visible (primarily  $D_{\alpha}$ ) light has allowed edge intermittency to be studied in greater detail than possible with statistical analysis of single-point data, such as that from probes. Until recently, the sensitivity of fast camera detectors required relatively long integration times to collect sufficient photons and the L-mode plasma edge tended to appear ‘diffuse’. The latest generation of cameras, however, can comfortably operate at rates up to  $10^5$  frames per second (integration times  $< 10 \mu\text{s}$ ). One such camera has been installed on MAST. A typical image from a beam heated L-mode plasma is shown in figure 7, in which filamentary structures are clearly visible. When individual

filaments first appear on the image they are already highly elongated, stretching between the two X-points in the double-null configurations, and are aligned to the magnetic field in the edge. In wide-angle mode, the camera is limited to 7,500 f.p.s., which is not sufficient to follow the evolution of the filaments. Sufficiently high frame rates can be accessed, however, by using a reduced frame such as that shown in figure 8.

The reduced frame in figure 8 encompasses the region around the reciprocating probe, the position of which is indicated by a black circle. One of the filaments is seen to interact with the probe, which was at  $r = 4\text{cm}$  at this time. This interaction corresponds to a spike in the  $j_{\text{sat}}$ , shown in the lower trace. In fact, every  $j_{\text{sat}}$  spike appears to be

correlated to interaction with a filament, which are clearly intimately linked to the intermittency discussed in section 2. The characteristics of the filaments have therefore been studied in some detail, using the fast camera and an edge Thomson scattering system recently commissioned on MAST.

By fitting calculated field lines to the filaments on sequential camera frames, it is possible to derive their effective toroidal mode number,  $n_{\phi}$  toroidal velocity,  $v_{\phi}$  and toroidal correlation length,  $L_{\phi}$ . Using a reduced frame centred around the X-point region, where the camera view is roughly parallel to the local field (e.g. see lower left hand corner of figure 7), additionally allows the radial correlation length,  $L_r$  and radial velocity,  $v_r$  to be derived. An assumption is made in this analysis, of course, that the visible light imaged by the camera is



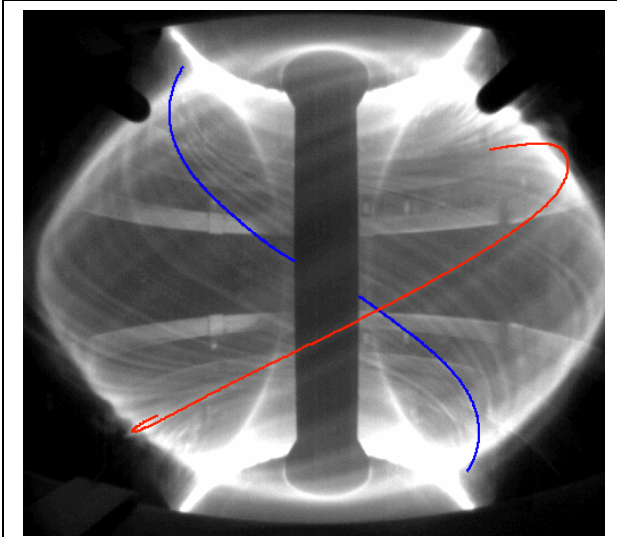


**Figure 7:** Wide angle image of a beam heated L-mode plasma in which filamentary structures are clearly visible. The filaments are elongated along field lines – which have been overlaid as red and blue curves on two of the filaments. The red curve is for a filament in the foreground and the blue curve for a filament on the opposite side of the plasma.

an accurate reflection of the size and dynamics of the filament. Figure 9 shows the distribution of  $n_\phi$  and  $L_\phi$  derived for a series of 1.2 MW beam heated L-mode plasmas in which the plasma current and toroidal field were varied (900 kA:0.54 T, 600 kA:0.54 T and 600 kA:0.45 T). The plasma density was  $2.6 \times 10^{19} \text{ m}^{-3}$  and the core temperature for the two 600 kA shots was 640 eV and 1.2 keV for the 900 kA shot. For this range of plasma parameters, no significant variation in either  $n_\phi$  or  $L_\phi$  was found, with the mean  $n_\phi$  being  $\sim 50 \pm 20$  and the mean  $L_\phi$  being  $0.1 \text{ m} \pm 0.04 \text{ m}$ .

As mentioned above, the filaments stretch between the X-points from their first appearance (e.g. localised ‘blobs’ are never observed), and thus have a parallel correlation length of  $\sim 10 \text{ m}$ . The filaments appear to rotate toroidally, in the co-current direction, with a broad distribution of  $v_\phi$  in the range 2 - 5 km/s. It cannot be ruled out from these measurements, however, that the motion could, in fact, be poloidal since toroidal and poloidal motion are indistinguishable in the camera view. Analysis of camera images from the X-point region gives  $L_r$  in the range 1 – 2 cm and  $v_r$  in the range 0.5 - 1.5 km/s. Typically, filaments can be followed over 2 to 6 frames whilst they expand radially and eventually dissipate. This corresponds to a lifetime of up to 60  $\mu\text{s}$ , consistent with the correlation timescale for Region I in figure 5. No clear correlation of filament parameters with plasma conditions has yet been established (although there is some evidence that  $n_\phi$  increases with edge density and  $L_\phi$  decreases).

The camera analysis is supported by data from a new, edge Thomson scattering system with  $\mu\text{s}$  time resolution (for four time points) and  $\sim 1 \text{ cm}$  spatial resolution, which shows spatially isolated peaks in density and temperature at the edge of L-mode plasmas, figure 10. These peaks are believed to be associated with the filaments. Maximum electron densities up to  $1 \times 10^{19} \text{ m}^{-3}$  are observed for peaks close to the separatrix and temperatures up to around 25 eV. These values are consistent with the filaments originating close to, or inside, the separatrix.

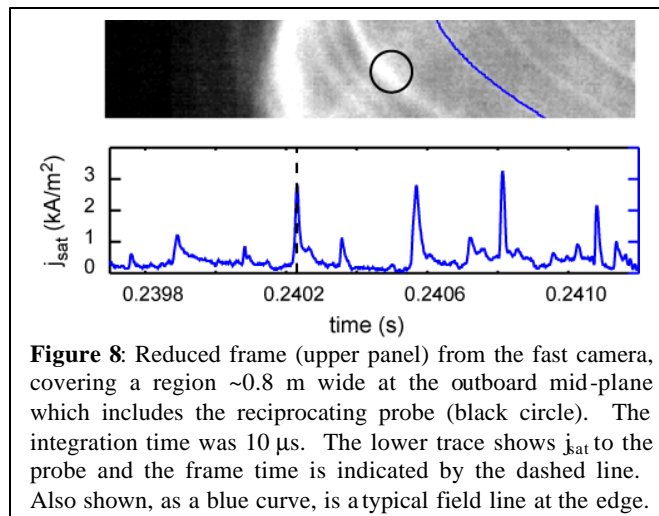


**Figure 8:** Reduced frame (upper panel) from the fast camera, covering a region  $\sim 0.8 \text{ m}$  wide at the outboard mid-plane which includes the reciprocating probe (black circle). The integration time was 10  $\mu\text{s}$ . The lower trace shows  $j_{\text{sat}}$  to the probe and the frame time is indicated by the dashed line. Also shown, as a blue curve, is a typical field line at the edge.

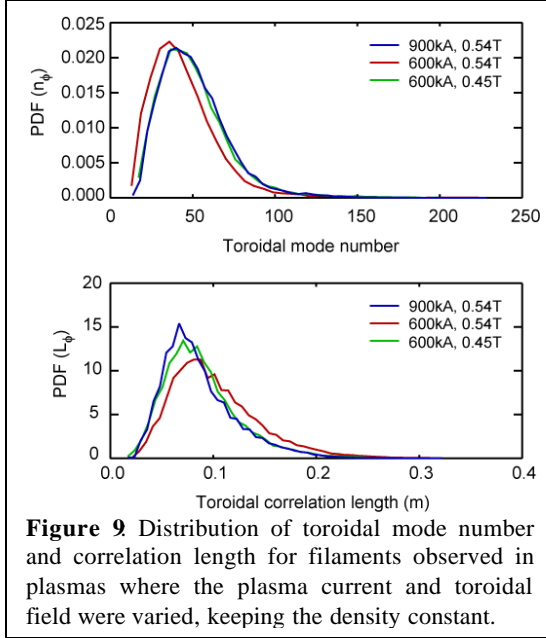


**Figure 9** Distribution of toroidal mode number and correlation length for filaments observed in plasmas where the plasma current and toroidal field were varied, keeping the density constant.

temperature by 15% (from 24eV to 26.5eV). There is also little change in the SOL 1/e fall-off length when compared to the ‘base level’ fall-off in L-mode (see figure 4). This is another indication that the filaments – at least those which make it to large  $r$  - are generated inside the separatrix in L-mode, close to the region in which there are large changes at the L-H transition (i.e. the pedestal).

### 5. Modelling of edge intermittency

The MAST edge plasma has been modelled using the two-fluid Braginskii code, BOUT [4] which has been adapted to double-null geometry. BOUT includes both closed and open field lines, as well as the magnetic x-point. In the radial-poloidal plane, the solution is obtained on a grid based on an EFIT reconstruction. The code has sources of many ideal and non-ideal instabilities which can lead to turbulence of both electromagnetic and electrostatic origin. Due to several specific features of spherical tokamaks, the time-step used in the code must be smaller than for a conventional tokamak, which makes observing saturated turbulence on long timescales quite challenging. Nevertheless runs of the code have now been successfully conducted for periods equivalent to  $> 1$  ms, sufficient for analysis of intermittency on timescales less than 400  $\mu$ s (see figure 4 and text). A sample of this analysis is presented in this section for a 500 kA Ohmic L-mode plasma with line averaged density of  $3 \times 10^{19} \text{ m}^{-3}$ .

Elongated, field-aligned turbulent fluctuations in density (figure 12) and temperature are clearly seen to evolve in the code runs driven by electrostatic drift-wave turbulence. The fluctuations have radial correlation lengths similar to those observed experimentally (1 - 2 cm). The mean number of toroidally distributed peaks in the density at a given radius

### 4. Intermittency at the L-H transition

L-H transitions observed with reciprocating probes show a rapid, and complete cessation in intermittent activity over a period of a few hundred microseconds. Even probes very close to the separatrix (5 mm) see fluctuation levels in the particle flux reduced by more than two orders of magnitude, figure 11. No filaments are observed in the SOL using the camera and visible light emission is limited to a sharp, constant band near the separatrix. This dramatic change in SOL intermittency, is not accompanied by a similar change in plasma parameters. Compared to the large changes occurring in the pedestal region, the separatrix density changes by only 20% (from  $5 \times 10^{19} \text{ m}^{-3}$  to  $6.3 \times 10^{19} \text{ m}^{-3}$ ) for the L-H transition shown in figure 11 and the

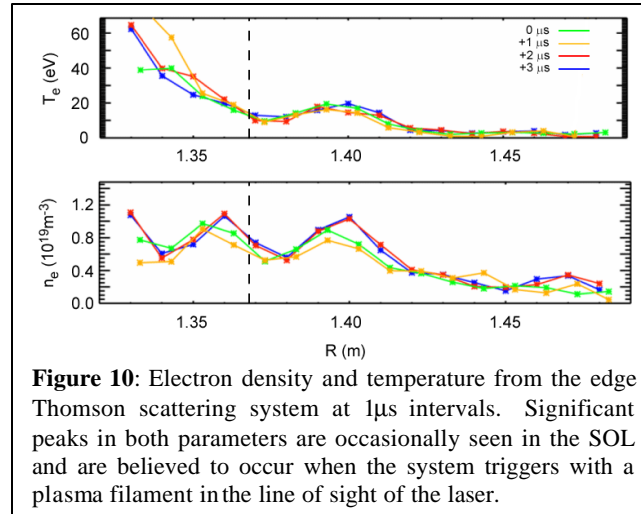
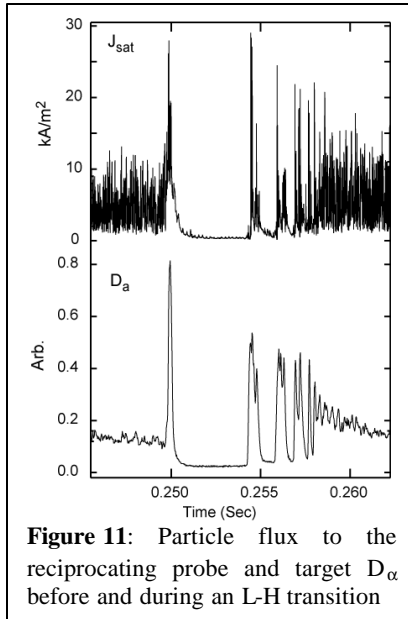


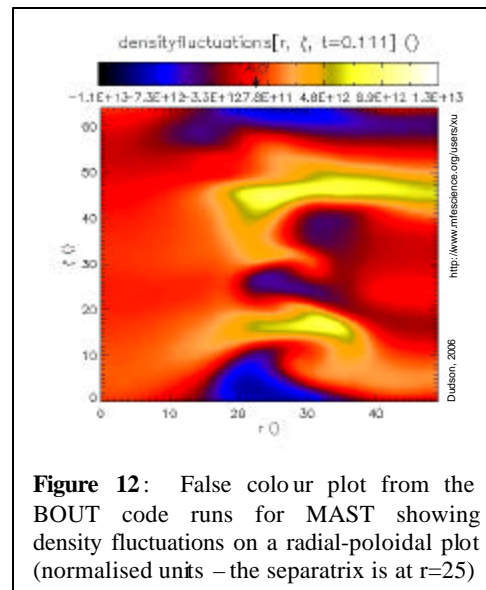
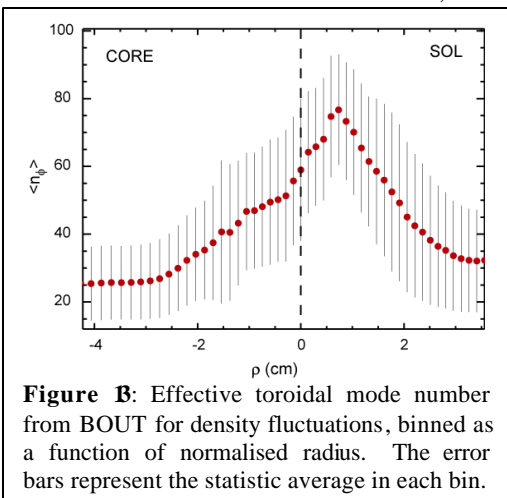
**Figure 10:** Electron density and temperature from the edge Thomson scattering system at 1 $\mu$ s intervals. Significant peaks in both parameters are occasionally seen in the SOL and are believed to occur when the system triggers with a plasma filament in the line of sight of the laser.



is shown in figure 13. Very high mode numbers occur within a centimetre or so of the separatrix but fall off quickly to  $n_\phi \sim 30 - 40$  further out in the SOL and towards the core. The mode numbers are broadly consistent with observations. Starting from a stationary plasma, these filaments develop a co-current rotation falling from  $\sim 9$  km/s at 3 cm inside the separatrix to  $\sim 3$  km/s just outside the separatrix, again consistent with observations.

Figure 14 shows a plot of fluctuations in the square of the parallel velocity and in the density as a function of  $r$ . The mean parallel velocity squared is a measure of the kinetic energy in turbulent eddies, which peaks around the separatrix. The density fluctuations however are highest just outside the separatrix ( $\sim 5$  mm). In both cases the levels decline and level off around 1 - 2 cm from the separatrix.

The figure shows that there is a peak in the turbulent mixing of eddies between  $-1 \text{ cm} < r < 0.5 \text{ cm}$ , which tails off further out into the SOL. This turbulent mixing would be expected to result in more symmetric, less skewed PDFs near to and inside the separatrix, as observed, since it will produce both positive and negative deviations around a 'background' level. In the SOL, large density fluctuations ejected radially outwards from the edge region produce the positively skewed distributions. The origin of the drive for this ejection is hinted at in figure 15, which shows the magnitude of the advection and curvature drive terms. Inside the separatrix radial advection by ExB velocity dominates, but this tails off rapidly on the SOL. Curvature drive terms, however, reach a peak and plateau in the SOL. Here it should be noted that the absolute magnitude of the drive term does not correspond directly to the ejection velocity and that the relationship is different in the advection and curvature drive cases. In the SOL it is expected that the curvature drive will actually dominate due to rapid dissipation local electric fields. One credible hypothesis, therefore, is that density fluctuations arising from turbulent mixing of eddies in a region of electrostatic drift-wave turbulence are ejected by curvature drive into the SOL (as for interchange turbulence).



## 6. Discussion and conclusions

Plasma with L-mode edge would form an

attractive operating scenario in a future fusion power plant. A better understanding of transport in the L-mode edge, through improved diagnostic measurements and the current generation of advanced models, is therefore very relevant – for example to allow static heat loads in future devices to be predicted with some confidence. In MAST, as on all tokamaks, the most obvious feature of the L-mode edge is the strong intermittency in plasma parameters. A range of statistical techniques; probability density functions, structure function analysis, conditional averaging, have been used to characterise this intermittency on MAST. PDFs for fluctuations with short timescale correlation ( $< 60 \mu\text{s}$ ) and for parameters in the ‘far’ SOL ( $r > \sim 1 - 2 \text{ cm}$ ) are very similar, as are the PDFs for long timescale fluctuations ( $> 60 \mu\text{s}$ ) and parameters near the separatrix ( $r < \sim 0.5 \text{ cm}$ ). Fast

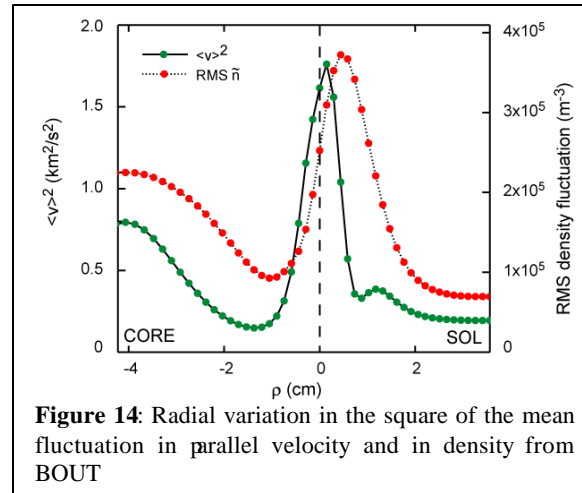


**Figure 14:** Radial variation in the square of the mean fluctuation in parallel velocity and in density from BOUT

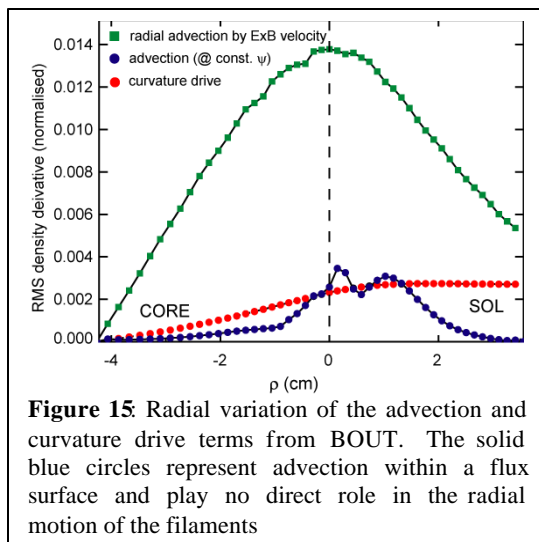


**Figure 15:** Radial variation of the advection and curvature drive terms from BOUT. The solid blue circles represent advection within a flux surface and play no direct role in the radial motion of the filaments

camera and edge Thomson scattering systems show that the fluctuations in the ‘far’ SOL are directly correlated to the radial and toroidal propagation of field-aligned, highly elongation plasma filaments. The size (toroidal, radial and parallel correlation lengths) and dynamics (toroidal/poloidal and radial velocities, correlation timescale) have been characterised. Modelling of the edge plasma has been conducted using the BOUT code, modified for use in the MAST double-null geometry. The results are broadly consistent with the experimental observations and suggest that density fluctuations driven by mixing of eddies arising from electrostatic drift-wave turbulence are ejected outwards into the SOL by curvature drive.

This work was funded jointly by the United Kingdom Engineering and Physical Sciences Research Council and by the European Communities under the contract of Association between EURATOM and UKAEA. The views and opinions expressed herein do not necessarily reflect those of the European Commission

- [1] B A Carreras et. al., Phys. Plasmas 8 (2001) 3702
- [2] C Hidalgo et. al., Plasma Phys. Control. Fusion 37 (2001) A53
- [3] S Krasheninnikov, Phys. Lett. A 283 (2001) 368
- [4] BOUT documentation and publications: <http://www.mfescience.org/users/xu>
- [5] J P Graves, J Horacek, R A Pitts and K I Hopcraft, Plasma Phys. Control. Fusion 47 (2005) L1
- [6] D L Rudakov et. al., Plasma Phys. Control. Fusion 44 (2002) 717
- [7] Y H Xu, S Jachmich and R R Weynants, Plasma Phys. Control. Fusion 47 (2005) 1841
- [8] B Ph VanMilligan et. al., Phys. Plasmas 12 (2005) 052507
- [9] G Y Antar, G F Counsell, Y Yu, B LaBombard and P Devynck, Phys. Plasmas 10 (2003) 419
- [10] B D Dudson, R O Dendy, A Kirk, H Meyer and G F Counsell, Plasma Phys. Control. Fusion 47, 885 (2005)
- [11] B Hnat, B D Dudson, R O Dendy, G F Counsell and A Kirk, ‘Characterisation of edge turbulence in L-mode plasmas in the Mega Amp Spherical Tokamak’, 33<sup>rd</sup> EPS Conference, Rome, (2006)